Semiconductor Physics, Quantum Electronics & Optoelectronics, 2026. V. 29, No 2. P. 153-161.

Semiconductor physics

Structural evolution of Fe/Pt multilayered films annealed in different atmospheres: a synchrotron radiation study

O.A. Palchekovskyi*, I.O. Kruhlov, R.V. Pedan, I.A. Vladymyrskyi, A.K. Orlov

National Technical University of Ukraine "Igor Sikorsky Kyiv Polytechnic Institute", 37 Beresteiskyi Avenue, 03056 Kyiv, Ukraine
**Corresponding author e-mail: palchekovskyi.oleksandr@lll.kpi.ua*

Abstract. Influence of annealing atmosphere on the structural properties of annealed multilayered $[Fe/Pt]_{\times 4}$ thin films was investigated. The films were deposited onto thermally-oxidized SiO_2(100nm)/Si(100) substrates by direct current magnetron sputtering at room temperature and subsequently annealed in a temperature range of 500 to 900 °C in flowing Ar, N_2, and $Ar + H_2$ atmospheres to induce structural phase transitions and chemical ordering. Synchrotron analysis revealed that ordered face-centered tetragonal $L1_0$-FePt phase formed after annealing at 500 °C regardless of the atmosphere used. Among the studied conditions, annealing in N_2 at 800 °C provided higher degree of chemical ordering, strong [001] crystallographic texture, and higher tetragonality of the $L1_0$-FePt phase, making the latter the most favorable for magnetic data storage applications. The surface roughness increased at rising the temperature. However, its magnitude also depended on the annealing atmosphere, being comparatively lower after annealing in Ar compared to treatment in reactive environments such as N_2 or $Ar + H_2$. Furthermore, annealing in Ar atmosphere promoted formation of a non-stoichiometric $Fe_{1+x}Pt_{3-x}$ solid solution and surface oxides ($Fe_3O_4 \rightarrow Fe_2O_3 \rightarrow FeO$) alongside with the $L1_0$-FePt phase.

Keywords: magnetic thin films, Fe–Pt alloy, synchrotron radiation, annealing atmosphere, oxidation behavior.

https://doi.org/10.15407/spqeo29.02.153
PACS 07.85.Qe, 75.70.-i, 81.15.Cd, 81.40.Ef

Manuscript received 20.10.25; revised version received 18.05.26; accepted for publication 10.06.26; published online 23.06.26.

1. Introduction

FePt thin films have been widely investigated over the last few decades for applications in perpendicular magnetic ultrahigh-density recording media [1–3], micro-electromechanical systems (MEMS) [4], and spintronic devices [5–7]. These applications benefit from the chemically ordered face-centered tetragonal (fct) $L1_0$-FePt phase, which exhibits high magnetocrystalline anisotropy ($K_u \approx 10^7$ erg/cm^3), high saturation magnetization (~1100 emu/cm^3), large coercivity, and excellent chemical stability [8–11].

However, achieving the $L1_0$ ordered structure occurs through formation of soft magnetic face-centered cubic (fcc) $A1$ structure, which is strongly affected by the deposition conditions. Therefore, to obtain films with the fct structure, deposition on a heated substrate or post-deposition annealing is required [12]. One of the promising approaches to synthesize chemically ordered $L1_0$-FePt phase is sequential deposition of individual Fe and Pt layers followed by thermal annealing [13, 14]. It is known that the structural and magnetic properties of FePt films are highly sensitive to the annealing conditions such as temperature, duration, heating rate, *etc*. Furthermore, the annealing environment has a pronounced effect on the grain size, crystallographic texture, ordering, and surface morphology of the FePt-based films. For instance, annealing in forming gas ($Ar + H_2$) significantly enhances coercivity and promotes $L1_0$ ordering at reduced temperatures due to hydrogen incorporation into interstitial sites [15]. Similarly, annealing in pure H_2 facilitates development of the [001] texture. In addition, annealing in H_2 atmosphere has been shown to reduce oxygen incorporated during deposition, leading to significantly higher magnetization. Moreover, hydrogen promotes phase formation, initiates $L1_0$ ordering at temperatures as low as 350 °C, and simultaneously suppresses grain growth, resulting in a coercivity as high as 1.1 T after annealing at 600 °C [16]. In contrast, annealing in N_2 often leads to surface oxidation and composition modifications [17]. Nitrogen atoms can also segregate at the grain boundaries, hindering grain growth but simultaneously accelerating atomic diffusion [18]. Finally, the films annealed in nominally inert gases, such as Ar or N_2, are highly sensitive to presence of residual oxygen, which may drastically affect the ordering process and the grains' crystallographic orientation [19].

Therefore, the mentioned studies emphasize that annealing atmosphere strongly influences structural and magnetic properties of $L1_0$-FePt films. However, the existing findings provide no clear guidance on the optimal choice of annealing atmosphere, temperature conditions, or their combination. Therefore, this work is devoted to a thorough synchrotron structural analysis of multilayered $[Fe/Pt]_{\times 4}$ films annealed at temperatures in the range of 500 to 900 °C in different atmospheres (N_2, Ar, and forming gas (97% Ar + 3% H_2)). This approach provides a comprehensive insight into the influence of different annealing atmospheres on ordering of FePt-based structures.

2. Experimental

$[Fe(3.2\ nm)/Pt(4.2\ nm)]_{\times 4}$ multilayered films were deposited by direct current magnetron sputtering onto thermally-oxidized Si(001) substrates with a 100-nm-thick amorphous SiO_2 layer at room temperature. Before the deposition, the Si substrates were subjected to a multi-step wet chemical cleaning procedure developed by the Radio Corporation of America (RCA). Fe and Pt layers were deposited from individual high-purity Fe (99.9%) and Pt (99.95%) targets. All the depositions were carried out under Ar sputtering at the pressure of 0.35 Pa, while the base pressure was $5 \cdot 10^{-5}$ Pa. The individual layer thicknesses were adjusted to achieve equiatomic stoichiometric composition of the annealed product phase and were verified by Rutherford backscattering spectroscopy.

After the deposition process, the films were subjected to annealing at 500…900 °C in Ar, N_2, and Ar + H_2 (3 vol.%) atmospheres at a constant gas flow rate of 0.2 L/min. The annealing was conducted for 30 s at each temperature using a fixed heating rate of 10 °C/s.

Structural characterization of the annealed films was performed at the SPring-8 synchrotron radiation facility using the RIKEN Materials Science beamline BL44B2 [20, 21]. Grazing-incidence wide-angle X-ray scattering (GIWAXS) and X-ray reflectivity (XRR) measurements were carried out at an incidence angle of 0.5° relative to the sample surface, employing X-rays with a wavelength of 0.108 nm. The vertical and horizontal beam sizes were adjusted to 0.01 and 3.0 mm, respectively. The samples were mounted in a Debye–Scherrer camera equipped with a 2D image plate detector (400 × 200 mm) enabling data acquisition over a 2θ range from 2° to 78° with a step of 0.01°. Fig. 1 shows a schematic illustration of the used GIWAXS measurement setup.

Lattice parameters and relative peak intensities were calculated by Rietveld refinement using Rigaku PDXL 2 software. The refinement was performed with a polynomial background function, axial displacement peak shift correction, and a split pseudo-Voigt peak shape model. The effects of preferred orientation of grains were accounted for using the March–Dollase function to improve the accuracy of lattice parameter determination. To evaluate the film texture, the intensity ratios of (001)/(111) peaks were determined from the relative peak intensities obtained from PDXL analysis without

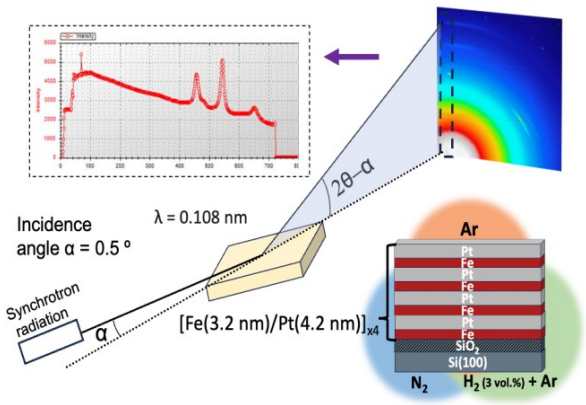

Fig. 1. Schematic illustration of GIWAXS measurements on the BL44B2 beamline.

applying preferred orientation correction. The degree of chemical ordering of the $L1_0$-FePt phase was estimated from the intensity ratio of the (001) superlattice to the (002) fundamental peaks. The crystallite sizes were determined using the Williamson–Hall method [22]. Deconvolution of the asymmetric (001) and (111) peaks was performed using Gaussian fitting. X-ray reflectivity simulations with varying surface roughness were carried out using Rigaku GlobalFit software. The model included a FePt film (29.6 nm) deposited on a SiO_2(100 nm)/Si substrate and used the bulk density value of 15.48 g/cm³.

3. Results and discussion

Figs. 2–4 show XRD patterns of $[Fe/Pt]_{\times 4}$ multilayered films annealed at different temperatures (500, 600, 700, 800, and 900 °C) in N_2, Ar + H_2, and Ar atmospheres plotted in the 10°…75° 2θ range.

Annealing in N_2 and Ar + H_2 atmospheres suggests predominant formation of a single-phase chemically ordered fct $L1_0$-FePt (PDF #03-065-9121) structure, indicating complete thermally-induced ordering of the film. The diffraction peaks corresponding to other intermetallic phases were not detected. In contrast, annealing in an Ar atmosphere, except for formation of the $L1_0$-FePt phase, leads to the film oxidation. Specifically, Fe_3O_4 (magnetite) oxide with Fd-3m structure was detected after annealing at 500…700 °C. At 800 °C, diffraction peaks corresponding to Fe_2O_3 (hematite, R-3c) and probably PtO_2 (Pn-3m) were detected. Finally, at 900 °C, formation of FeO (wüstite) with the Fm-3m structure became dominant. The formation of iron oxides in the Ar atmosphere may be attributed to the high chemical reactivity of Fe atoms towards residual oxygen at elevated temperatures. Even under flowing inert or forming gas, oxygen impurities cannot be completely eliminated from the annealing chamber, resulting in surface oxidation of the film [23–25]. The observed sequence of oxides formation is supported by the expected thermodynamic constants of respective reactions. In particular, Fe_3O_4 (–1123 kJ/mol) has a lower formation enthalpy compared to Fe_2O_3 (–829 kJ/mol) and FeO (–267 kJ/mol) [26].

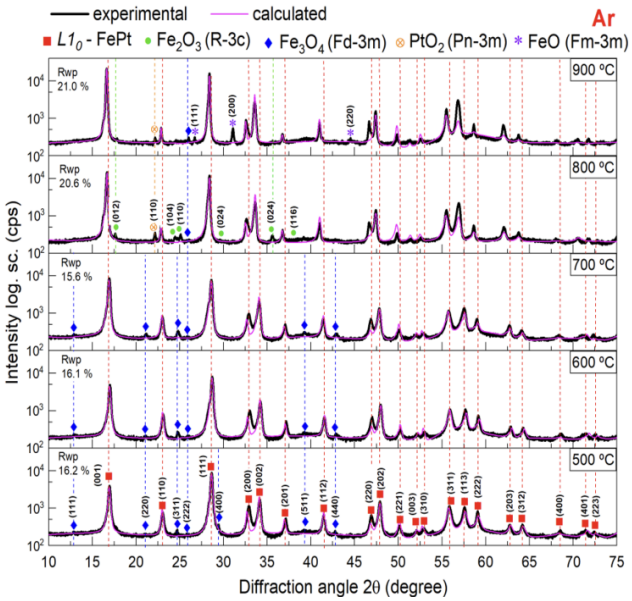

Fig. 2. XRD patterns of the $[Fe/Pt]_{\times 4}$ multilayered films annealed in Ar atmosphere at temperatures ranging from 500 to 900 °C.

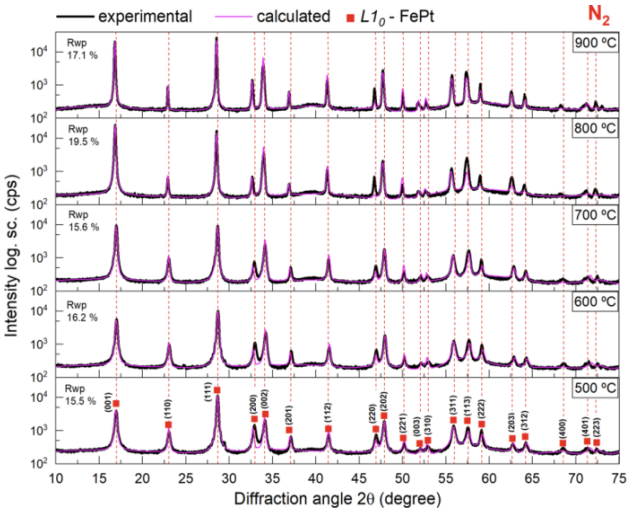

Fig. 3. XRD patterns of the $[Fe/Pt]_{\times 4}$ multilayered films annealed in N_2 atmosphere at temperatures ranging from 500 to 900 °C.

Therefore, this progressive evolution from magnetite to hematite and ultimately to wüstite correlates with increasing annealing temperatures and is consistent with the energies of Fe oxides formation. Film oxidation can significantly degrade magnetic properties by disrupting formation of the $L1_0$ phase and depleting Fe from the bulk of the film. In contrast, hydrogen-containing environments are capable of reducing the surface iron oxide [27, 28] due to the capability of hydrogen to react with oxygen. During annealing in N_2 atmosphere, nitrogen atoms can be predominantly incorporated at grain boundaries [18] leading to inhibition of the oxidation process at the subsurface region [29].

Moreover, annealing in Ar, as compared to N_2 and Ar + H_2 atmospheres, exhibits noticeable asymmetry of the (001) superstructure and (111) fundamental peaks,

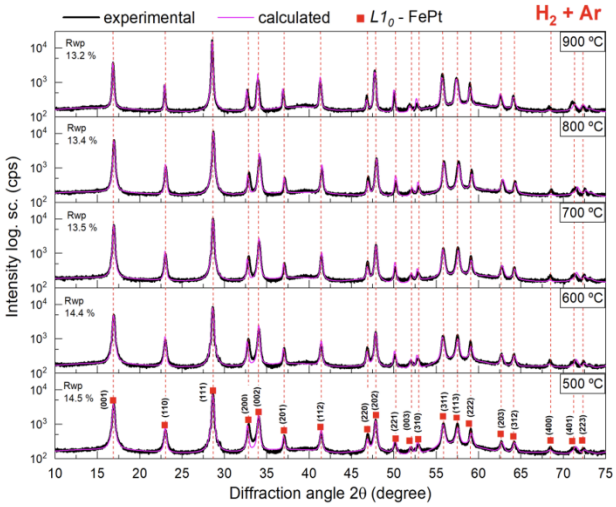

Fig. 4. XRD patterns of the $[Fe/Pt]_{\times 4}$ multilayered films annealed in Ar + H_2 atmosphere at temperatures ranging from 500 to 900 °C.

spotted at 16.95° and 28.64°, respectively (Fig. 5). The observed shoulder at the lower-angle sides at 16.5° and 28.25° may be attributed to the presence of the Pt-rich $FePt_3$ phase with the $L1_2$ structure. Formation of this non-equiatomic phase may be attributed to the existence of near-surface areas with iron deficiency: oxidation during annealing results in selective consumption of Fe atoms to form surface oxides (*e.g.*, Fe_3O_4, Fe_2O_3, FeO). However, the theoretical positions of the (001) and (111) peaks from $FePt_3$ (16.04° and 27.97° (PDF #01-077-7991)) are at slightly lower angles than those observed experimentally. According to the Vegard's law, the lattice parameter of a binary solid solution linearly varies with the atomic percents of its constituents. Hence, the observed peak shift may instead be attributed to formation of a non-stoichiometric $Fe_{1+x}Pt_{3-x}$ solid solution with $0 < x < 1$. Furthermore, within the temperature range of 500 to 700 °C, distinct Laue oscillations were detected in the vicinity of the (001) and (111) diffraction peaks for the thin film annealed in Ar atmosphere. Presence of the Laue oscillations may indicate (i) high degree of structural coherence over the entire film thickness, (ii) smooth and planar interfaces between the film and the substrate/environment, and (iii) homogeneity of the grown films [30–33]. However, the intensity and sharpness of the oscillations gradually decrease with increasing annealing temperature, suggesting degradation of the interface quality and increase in the surface roughness. At higher temperatures (800 and 900 °C), the Laue oscillations completely disappear, indicating loss of structural coherence, which may be attributed to roughening of the interface between the film and the substrate and/or the environment. Similar distortions are also observed after annealing in N_2 and Ar + H_2 atmospheres already at 500 °C, indicating that the film annealed in Ar is characterized by smoother and more planar interfaces up to a temperature of 800 °C compared to the other investigated atmospheres.

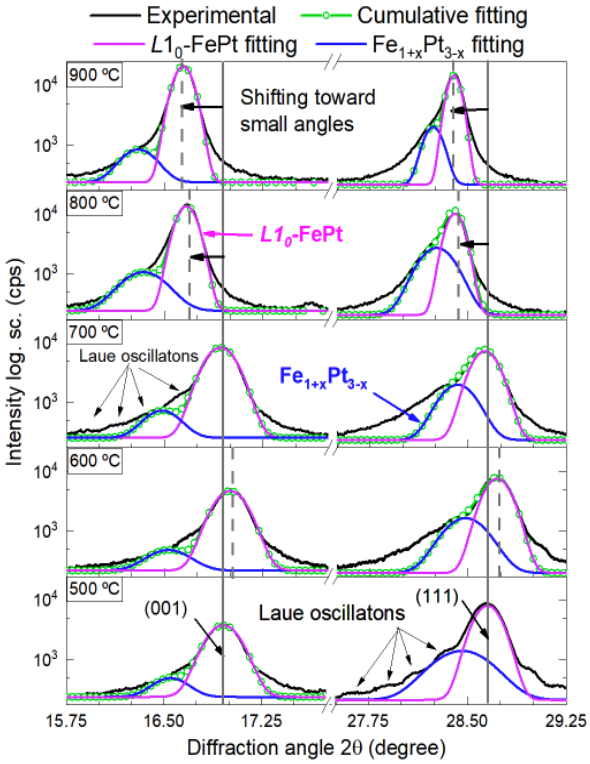

Fig. 5. Enlarged XRD patterns of the $[Fe/Pt]_{\times 4}$ multilayered films annealed in Ar atmosphere in a temperature range from 500 to 900 °C, showing (001) and (111) deconvolved peaks.

Rietveld refinement was performed to determine precisely the behavior of the structural properties of the annealed films. The simulated curves (pink lines) and corresponding *R*-factors (R_{wp} values) are shown in Figs. 2–4. The summarized structural parameters, including crystallite size, tetragonality degree (*c*/*a* lattice constants ratio), the (001)/(111) and (001)/(002) integrated intensity ratios are plotted in Fig. 6 as functions of the annealing temperature for various used atmospheres.

The crystallite size as a function of annealing temperature for different atmospheres is shown in Fig. 6a. For all the annealing atmospheres, a clear trend to recrystallization-driven grain growth at increasing the annealing temperature is observed. The most pronounced crystallite growth from 15 nm at 500 °C to ~46 nm at 900 °C occurs in N_2 atmosphere, which may correlate with enhanced atomic diffusion. Previous studies have reported that nitrogen atoms can occupy interstitial sites within the FePt lattice, thereby inducing substantial in-plane compressive strain and consequently reducing the thermodynamic driving force for (111)-oriented grain growth [34]. In contrast, in the present study, elevated annealing temperatures promote rapid out-diffusion of nitrogen atoms from the FePt phase. This degassing process leads to the formation of numerous nanoscale voids within the film, which, in turn, enhance the diffusivity of Fe and Pt atoms and facilitate accelerated grain growth [35]. In its turn, H_2 atmosphere leads to growth of crystallites from 15 nm at 500 °C to ~28 nm at 900 °C, which is less pronounced compared to annealing in N_2. This may be attributed to segregation of hydrogen atoms at grain boundaries [36, 37]. Unlike nitrogen, hydrogen atoms tend to block the boundaries movement [37], thereby slowing down the grain growth.

Fig. 6b shows the evolution of the tetragonality degree of the $L1_0$-FePt phase with annealing temperature. In the Ar + H_2 atmosphere, the *c*/*a* ratio remains stable across the entire temperature range. It closely matches with the bulk $L1_0$ value of 0.964 (indicated by the solid line), suggesting preservation of an ordered tetragonal phase. In contrast, more pronounced deviations from the bulk value are observed for Ar and N_2 atmospheres. The smaller values of the *c*/*a* ratio are registered after annealing at 600 °C in Ar and 700 °C in N_2, which indicates a higher degree of chemical ordering [38].

The ratio of the integral intensities of the superlattice (001) peak to the fundamental (111) one provides insights into the out-of-plane texture of the FePt films (Fig. 6c). For the $L1_0$-FePt structure with randomly oriented grains, the theoretical (001)/(111) intensity ratio is approximately equal to 0.25 [39]. After treatment in Ar atmosphere, this ratio increases with annealing temperature, indicating progressive reorientation of the grains along the [001] direction. A similar trend is observed after annealing in N_2 up to 800 °C, when this ratio reaches a maximum, likely reflecting optimal conditions for film texturing. However, annealing at 900 °C results in a noticeable decrease in preferred grains orientation. In contrast, annealing in Ar + H_2 atmosphere leads to decrease of the (001)/(111) ratio within the entire temperature range, suggesting that hydrogen-containing environments suppress development of out-of-plane texture.

Fig. 6d demonstrates the ratio of the integrated intensities of the superlattice (001) peak to the fundamental (002) one, which is proportional to the degree of chemical ordering of the $L1_0$-FePt structure. In the case of Ar atmosphere, this ratio steadily increases with temperature, reaching a maximum at 900 °C. For the N_2 atmosphere, the ordering enhances with temperature up to 800 °C and further decreases possibly due to film degradation. In contrast, annealing in Ar + H_2 atmosphere results in a nearly constant (001)/(002) ratio that is significantly lower compared to that for other two investigated atmospheres, indicating suppressed ordering. These results align with the previously reported observations that reduction (containing H_2) atmospheres inhibit structure ordering [37].

The XRR spectra of the $[Fe/Pt]_{\times 4}$ thin films annealed at different temperatures in Ar, N_2, and Ar + H_2 atmospheres are shown in Fig. 7a–7c. In all cases, absence of strong Bragg reflections indicates that compositional homogeneity has been achieved during annealing [13].

Moreover, small and closely spaced oscillations are observed after the treatment at 500…700 °C in Ar atmosphere, and 500 °C and 600 °C in N_2 and Ar + H_2, respectively. Since these features are associated with interaction of waves reflected from the film/ambient and the film/substrate interfaces, they can be used for roughness estimation. For this reason, XRR simulations in GlobalFit were performed. Fig. 7d shows the simulated XRR curves for FePt films with the same total

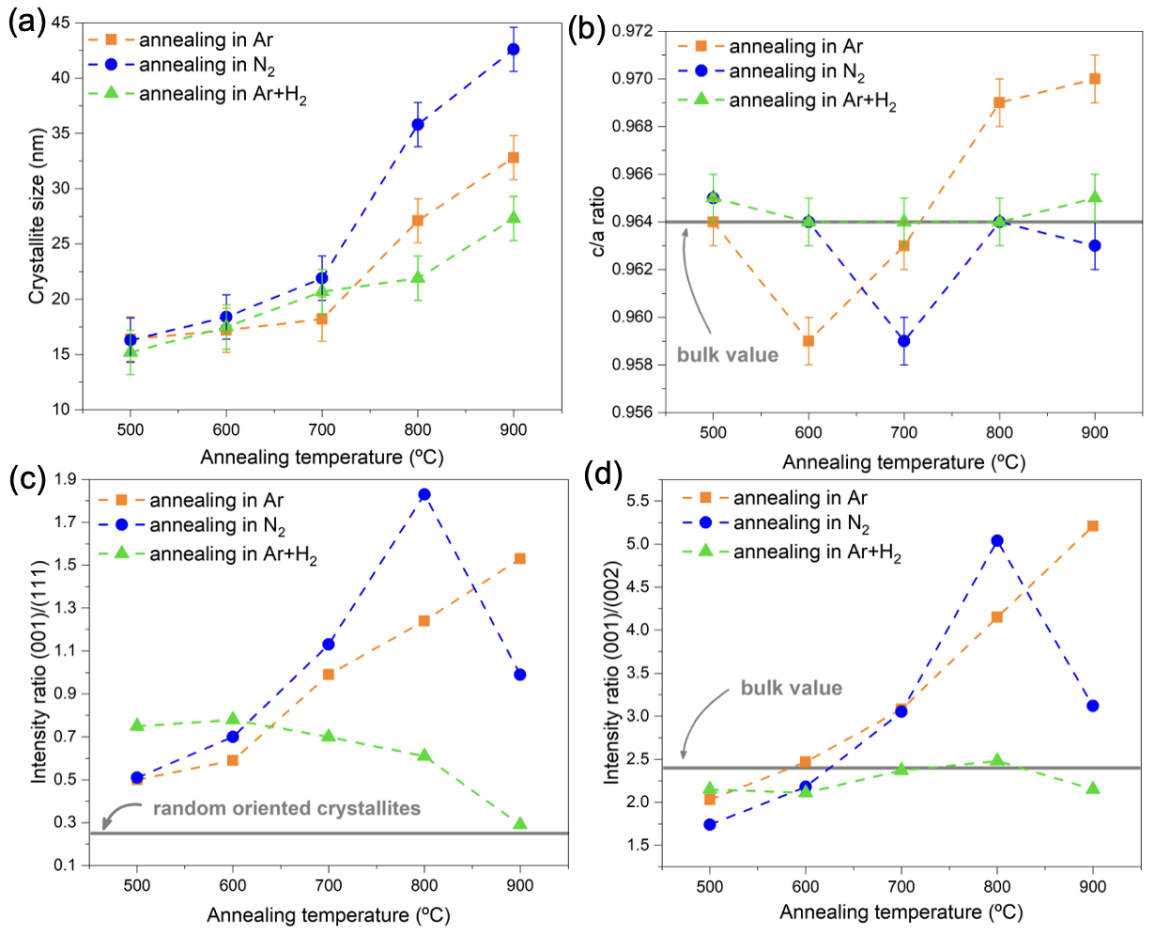

Fig. 6. Dependence of the (a) crystallite size, (b) tetragonality (*c*/*a* ratio), (c) integral intensity ratio of the (001) to (111) peaks, and (d) integral intensity ratio of the (001) to (002) peaks for the $L1_0$-FePt phase on the temperature of annealing in different atmospheres.

thickness and different surface roughness. The results indicate that increasing the roughness leads to progressive damping of these small oscillations. In general, surface roughness increases with temperature in all atmospheres. However, the film annealed at 700 °C in Ar retains more pronounced oscillations than those annealed in N_2 or Ar + H_2, indicating smoother surface under these conditions. This finding is consistent with the presence of Laue oscillations near the (111) and (001) diffraction peaks observed for the Ar atmosphere at 500…700 °C and confirms the smoother and more planar interfaces.

Considering all the results discussed above, the annealing atmosphere plays a vital role in the structural evolution of multilayered FePt-based films. At elevated temperatures, surface degradation and increased roughness are commonly observed phenomena. However, among the studied conditions, annealing in pure Ar atmosphere at 700 °C results in smoother film surfaces, as evidenced by the persistence of Laue oscillations. This suggests enhanced thermal stability under these conditions, likely due to formation of a thin crystalline oxide layer that inhibits further degradation. The smallest crystallite sizes are observed in the films annealed in Ar + H_2 atmosphere, while the largest crystallites are obtained by annealing in N_2. Smaller crystallites are preferable for high-density magnetic recording, as they reduce magnetic switching volumes and improve signal-to-noise ratios. The higher $L1_0$ chemical ordering and [001] texture development are observed after annealing in N_2 atmosphere at 800 °C. The reduction atmospheres such as Ar + H_2 suppress ordering and development of out-of-plane [001] texture, which are crucial for achieving high magneto-crystalline anisotropy.

These trends, including the changes of the crystallite size, tetragonality, ordering, texture, and surface roughness as functions of annealing temperature, are summarized in the schematic illustration shown in Fig. 8.

The influence of annealing atmosphere on structural transformations in FePt-based multilayered films is highlighted. For applications requiring strong perpendicular magnetic anisotropy, use of N_2-containing atmosphere and moderate annealing temperatures (*e.g.*, 800 °C) provides the most favorable balance of high ordering, texture, and grain size control. Meanwhile, Ar atmosphere may be advantageous where improved surface preservation and thermal stability are prioritized. These findings underline the critical role of annealing atmosphere in tuning the micro- and atomic structure of FePt thin films for magnetic device applications.

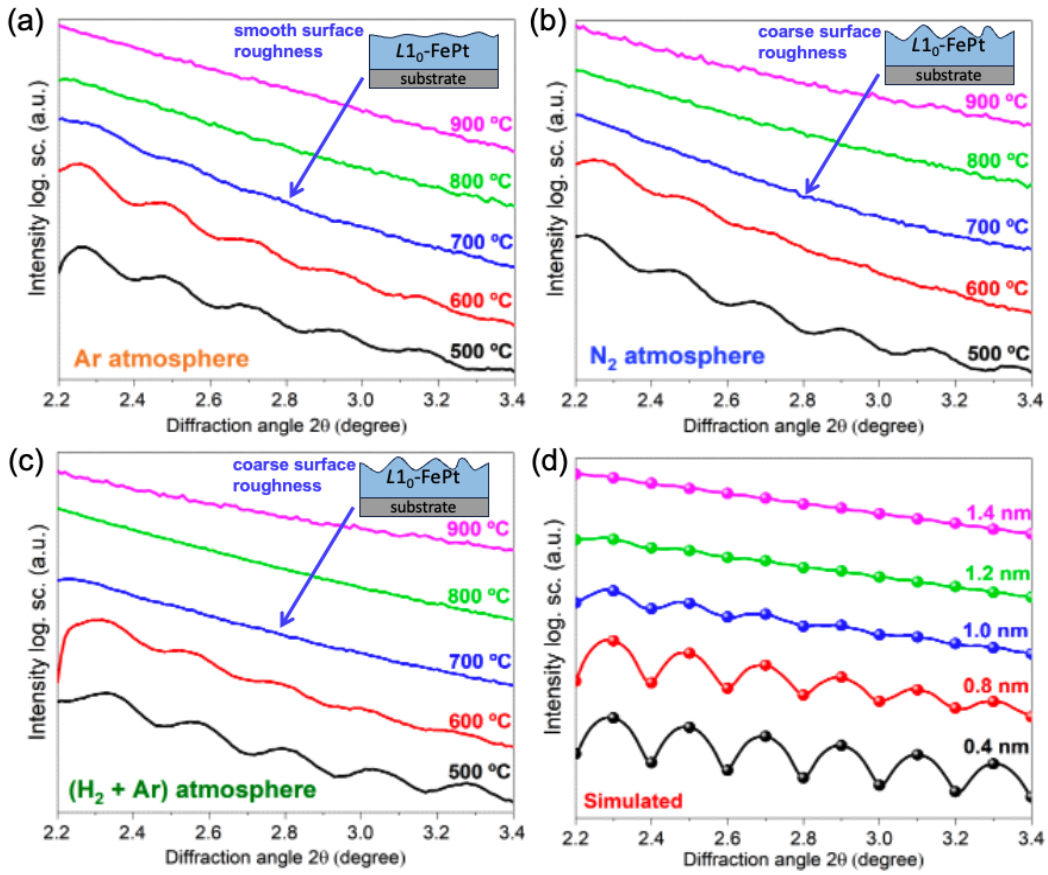

Fig. 7. XRR patterns of the $[Fe/Pt]_{\times 4}$ multilayered films annealed at different temperatures in (a) Ar, (b) N_2, and (c) H_2 + Ar atmospheres. (d) Simulated XRR curves of FePt films with different surface roughnesses.

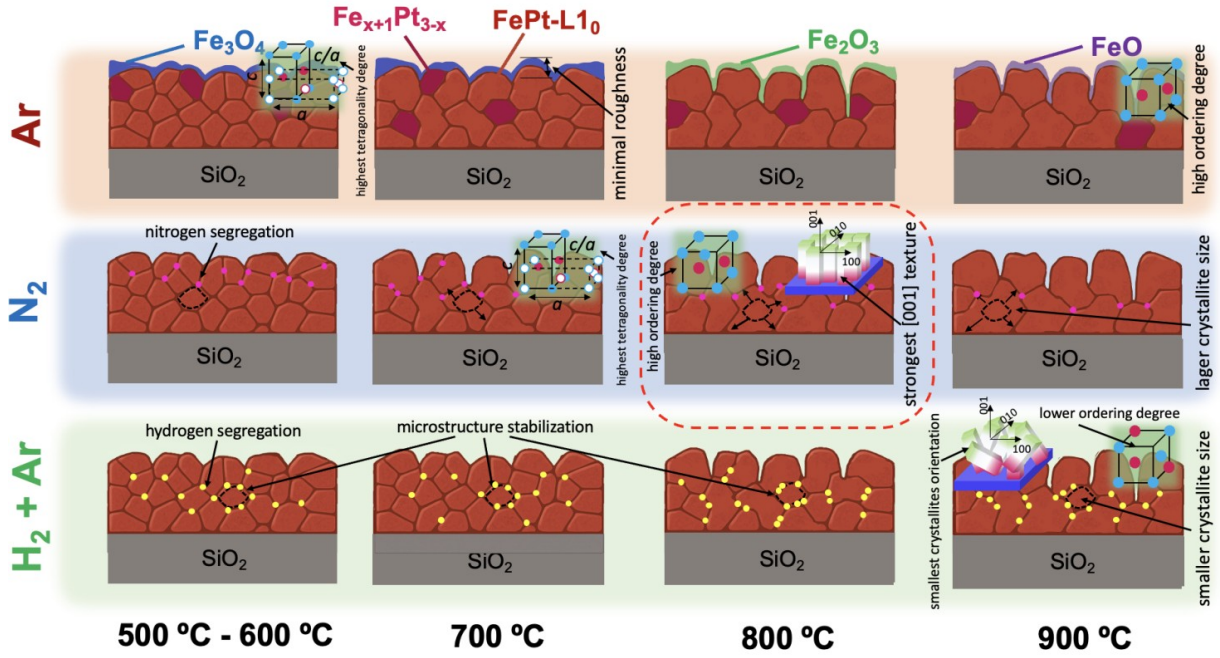

Fig. 8. Schematic illustration of the change in the structural parameters of the $[Fe/Pt]_{\times 4}$ multilayered films upon thermal annealing.

4. Conclusions

Fe/Pt multilayered thin films exhibit great potential for high-density magnetic recording due to unique magnetic properties of the chemically ordered $L1_0$-FePt phase. However, diffusion-controlled formation of this phase requires post-deposition heat treatment of the as-synthesized multilayered films. The annealing atmosphere influences on the grain size, crystallographic texture, degree of ordering, and surface morphology of the FePt-based films. In the present work, structural parameters of multilayered $[Fe/Pt]_{\times 4}$ thin films after annealing in different atmospheres (Ar, N_2, and Ar + H_2) were investigated by grazing-incidence wide-angle X-ray scattering and X-ray reflectivity measurements using synchrotron radiation. The chemically ordered fct $L1_0$ phase was formed after annealing at 500 °C irrespective of the annealing atmosphere. Furthermore, annealing in Ar atmosphere leads to formation of a non-stoichiometric $Fe_{1+x}Pt_{3-x}$ solid solution and surface oxidation: $Fe_3O_4 \rightarrow Fe_2O_3 \rightarrow FeO$. It was found out that the crystallite size increases as a result of annealing in N_2 atmosphere, while only a slight growth is observed for the Ar + H_2 case. This is associated with different behaviors of H and N incorporated atoms. The surface roughness also depends on the annealing atmosphere: although there is a general trend of increase of the roughness with temperature, this effect is significantly suppressed in Ar ambient due to the presence of surface oxides. It has been demonstrated that annealing in N_2 atmosphere at 800 °C results in the highest tetragonality and chemical ordering degree, and a pronounced [001] texture of the $L1_0$-FePt phase. This regime can be considered the most appropriate for obtaining $L1_0$ thin films with promising potential for data-storage applications.

Acknowledgment

The work was supported by the Ministry of Education and Science of Ukraine (Projects 0123U101257 and 0124U001266).

The synchrotron radiation experiments were performed at the BL44B2 RIKEN beamline SPring-8 facility (Proposal Nos. 20140101 and 20150078). The authors would like to thank Dr. K. Kato for support with the synchrotron experiments.

References

1. Chiou J.-Y., Chang H.W., Chi C.-C. *et al*. $L1_0$ FePt films with optimal (001) texture on amorphous SiO_2/Si substrates for high-density perpendicular magnetic recording media. *ACS Appl. Nano Mater.* 2019. **2**, No 9. P. 5663–5673. https://doi.org/10.1021/acsanm.9b01192.
2. Sasaki Y., Suzuki I., Mandal R. *et al.* Thermal modulation of magnetization dynamics in nanometer-thick L10-FePt nanogranular and continuous films for high-density magnetic recording media. *ACS Appl. Nano Mater.* 2023. **6**, No 7. P. 5901–5908. https://doi.org/10.1021/acsanm.3c00283.
3. Wang J., Sepehri-Amin H., Takahashi Y.K. *et al.* Magnetic in-plane components of FePt nanogranular film on polycrystalline MgO underlayer for heat-assisted magnetic recording media. *Acta Mater*. 2019. **177**. P. 1–8. https://doi.org/10.1016/j.actamat.2019.07.017.
4. Hsiao S.-N. FePt thin films: Fundamentals and applications, in: *Reference Module in Materials Science and Materials Engineering*. Elsevier, 2016. https://doi.org/10.1016/b978-0-12-803581-8.02678-3.
5. Tao Y., Sun C., Li W. *et al.* Field-free spin-orbit torque switching in $L1_0$-FePt single layer with tilted anisotropy. *Appl. Phys. Lett.* 2022. **120**, No 10. P. 102405. https://doi.org/10.1063/5.0077465.
6. Hirohata A., Yamada K., Nakatani Y. *et al.* Review on spintronics: Principles and device applications. *J. Magn. Magn. Mater*. 2020. **509**. P. 166711. https://doi.org/10.1016/j.jmmm.2020.166711.
7. Hafarov A., Prokopenko O., Sidorenko S. *et al.* $L1_0$ ordered thin films for spintronic and permanent magnet applications. In: Kaidatzis A., Sidorenko S., Vladymyrskyi I., Niarchos D. (Eds). Modern Magnetic and Spintronic Materials. *NATO Science for Peace and Security Series B: Physics and Biophysics*. Springer, Dordrecht. 2020. P. 73–94. https://doi.org/10.1007/978-94-024-2034-0_4.
8. Weller D., Parker G., Mosendz O. *et al.* Review article: FePt heat assisted magnetic recording media. *J. Vac. Sci. Technol. B*. 2016. **34**. P. 060801. https://doi.org/10.1116/1.4965980.
9. Zhang L., Han K., Zhang X. *et al.* Effect of a high magnetic field on hard magnetic multilayered Fe-Pt alloys. *J. Magn. Magn. Mater*. 2019. **490**. P. 165533. https://doi.org/10.1016/j.jmmm.2019.165533.
10. White C.W., Withrow S.P., Sorge K.D. *et al.* Oriented ferromagnetic Fe-Pt alloy nanoparticles produced in Al_2O_3 by ion-beam synthesis. *J. Appl. Phys.* 2003. **93**. P. 5656–5669. https://doi.org/10.1063/1.1565691.
11. Weller D., Moser A., Folks L. *et al.* High K/sub u/ materials approach to 100 Gbits/in/sup 2/. *IEEE Trans. Magn.* 2000. **36**. P. 10–15. https://doi.org/10.1109/20.824418.
12. Yu Y.S., Li H.-B., Li W.L. *et al.* Structure and magnetic properties of magnetron-sputtered $[(Fe/Pt/Fe)/Au]_n$ multilayer films. *J. Magn. Magn. Mater.* 2010. **322**, No 13. P. 1770–1774. https://doi.org/10.1016/j.jmmm.2009.12.027.
13. Yao B., Coffey K. The influence of periodicity on the structures and properties of annealed [Fe/Pt]n multilayer films. *J. Magn. Magn. Mater.* 2008. **322**. P. 559–564. https://doi.org/10.1016/j.jmmm.2007.07.030.
14. Gulyás S., Katona G.L. Structural and phase transformations in Fe-Pd-Ag layered thin films by grain boundary diffusion. *Phys. Scr.* 2024. **99**, No 9. P. 095970. https://doi.org/10.1088/1402-4896/ad6d9f.
15. Lai C.-H., Wu Y.-C., Chiang C.-C. Effects of forming gas annealing on low-temperature ordering of FePt films. *J. Appl. Phys.* 2005. **97**, No 10. P. 10H305. https://doi.org/10.1063/1.1851888.
16. Leistner K., Thomas J., Schlörb H. *et al.* Highly coercive electrodeposited FePt films by postannealing in hydrogen. *Appl. Phys. Lett.* 2004. **85**, No 16. P. 3498–3500. https://doi.org/10.1063/1.1807958.

17. Wu P., Hu X., Qian J., Yuan J. Nonepitaxial growth of a (001) textured $L1_0$ Fe-Pt film in H_2 and N_2 annealing atmospheres. *Rare Met.* 2006. **25**. P. 260–264. https://doi.org/10.1016/s1001-0521(06)60050-8.
18. Phatak V., Gupta A., Reddy V.R. *et al.* Effect of addition of N on $L1_0$ transformation and atomic diffusion in FePt films. *Acta Mater.* 2010. **58**. P. 979–988. https://doi.org/10.1016/j.actamat.2009.10.014.
19. Vladymyrskyi I.A., Karpets M.V., Ganss F. *et al.* Influence of the annealing atmosphere on the structural properties of FePt thin films. *J. Appl. Phys.* 2013. **114**, No 16. P. 164314. https://doi.org/10.1063/1.4827202.
20. Kato K., Tanaka H. Visualizing charge densities and electrostatic potentials in materials by synchrotron X-ray powder diffraction. *Adv. Phys. X*. 2016. **1**. P. 55–80. https://doi.org/10.1080/23746149.2016.1142830.
21. Orlov A.K., Kruhlov I.O., Shamis O.V. *et al.* Synchrotron analysis of structure transformations in V and V/Ag thin films. *Vacuum*. 2018. **150**. P. 186–195. https://doi.org/10.1016/j.vacuum.2018.01.044.
22. Williamson G.K., Hall W.H. X-ray line broadening from filed aluminium and wolfram. *Acta Metall.* 1953. **1**, No 1. P. 22–31. https://doi.org/10.1016/0001-6160(53)90006-6.
23. Xiao T., Yang Q., Yu J., Z *et al.* Annealing condition effects on the structural properties of FePt nanoparticles embedded in MgO via pulsed laser deposition. *Nanomaterials.* 2021. **11**, No 1. P. 131. https://doi.org/10.3390/nano11010131.
24. Orlov A.K., Kruhlov I.O., Lozova A. *et al.* Effect of Ar annealing on diffusion and thermal stability of transition metal thin-film systems. *Metallophysics & Advanced Technologies*. 2022. **44**, No 6. P. 735–749. https://doi.org/10.15407/mfint.44.06.0735.
25. Kruhlov I.O., Orlov A.K., Dubikovskyi O. *et al.* Inhibition of interlayer diffusion and reduction of impurities in thin metal films by ion irradiation. *Mater. Today Commun.* 2022. **34.** P. 104977. https://doi.org/10.1016/j.mtcomm.2022.104977.
26. Lilova K.I., Xu F., Rosso K.M. *et al.* Oxide melt solution calorimetry of Fe^{2+}-bearing oxides and application to the magnetite-maghemite (Fe_3O_4–$Fe_{8/3}O_4$) system. *Amer. Mineralogist*. 2012. **97**, No 1. P. 164–175. https://doi.org/10.2138/am.2012.3883.
27. Vedantam T.S., Liu J.P., Zeng H., Sun S. Thermal stability of self-assembled FePt nanoparticles. *J. Appl. Phys.* 2003. **93**, No 10. P. 7184–7186. https://doi.org/10.1063/1.1558233.
28. Sun S., Zeng H. Size-controlled synthesis of magnetite nanoparticles. *J. Amer. Chem. Soc.* 2002. **124**, No 28. P. 8204–8205. https://doi.org/10.1021/ja026501x.
29. Arabczyk W., Narkiewicz U. Oxidation of the Fe(111) surface covered with carbon or nitrogen. *Surf. Sci.* 2000. **454–456**. P. 227–233. https://doi.org/10.1016/s0039-6028(00)00285-5.
30. Miller A.M., Lemon M., Choffel M.A. *et al.* Extracting information from X-ray diffraction patterns containing Laue oscillations. *Z. Naturforsch. B.* 2022. **77**. P. 313–322. https://doi.org/10.1515/znb-2022-0020.
31. Song Y., Li Z., Li H. *et al.* Epitaxial growth and characterization of high quality Bi_2O_2Se thin films on $SrTiO_3$ substrates by pulsed laser deposition. *Nanotechnology*. 2020. **31**, No 16. P. 165704. https://doi.org/10.1088/1361-6528/ab6686.
32. Shu X., Zhou J., Liu L. *et al.* Role of interfacial orbital hybridization in spin-orbit-torque generation in Pt-based heterostructures. *Phys. Rev. Appl*. 2020. **14**, No 5. P. 054056. https://doi.org/10.1103/physrevapplied.14.054056.
33. Xu J., Katoch J., Ahmed A.S. *et al.* Growth of uniform $CaGe_2$ films by alternating layer molecular beam epitaxy. *J. Cryst. Growth*. 2017. **460**. P. 134–138. https://doi.org/10.1016/j.jcrysgro.2016.12.102.
34. Gao T., Zhang C., Sannomiya T. *et al.* Effect of nitrogen upon structural and magnetic properties of FePt in FePt/AlN multilayer structures. *J. Vac. Sci. Technol. A.* 2014. **32**, No 5. P. 051506. https://doi.org/10.1116/1.4891562.
35. Wang H.Y., Mao W.H., Ma X.K. *et al.* Improvement in hard magnetic properties of FePt films by N addition. *J. Appl. Phys.* 2004. **95**, No 5. P. 2564–2568. https://doi.org/10.1063/1.1643785.
36. Oudriss A., Creus J., Bouhattate J. *et al.* Grain size and grain-boundary effects on diffusion and trapping of hydrogen in pure nickel. 2012. *Acta Mater.* **60**, No 19. P. 6814–6828. https://doi.org/10.1016/j.actamat.2012.09.004.
37. Orlov A.K., Zhabynska O.O., Vladymyrskyi I.A. *et al.* Diffusion of Au and its influence on the coercivity of $[FePt/Au/FePt]_{2x}$ thin films during annealing in different atmospheres. *Thin Solid Films*. 2018. **658**. P. 12–21. https://doi.org/10.1016/j.tsf.2018.05.021.
38. You C.Y., Takahashi Y.K., Hono K. Magnetic properties and microstructures of Fe–Pt thin films sputter deposited under partial nitrogen gas flow. *J. Appl. Phys.* 2005. **98**, No 1. P. 013902. https://doi.org/10.1063/1.1943509.
39. Gupta R., Medwal R., Sharma P. *et al.* Effect of Pt layers on chemical ordering in FePt thin films. *Superlattices Microstruct*. 2013. **64**. P. 408–417. https://doi.org/10.1016/j.spmi.2013.10.006.

Authors' contributions

Palchekovskyi O.A.: investigation, formal analysis, visualization, methodology, conceptualization, writing – original draft, writing – review & editing.

Kruhlov I.O.: formal analysis, investigation, funding acquisition, writing – review & editing.

Pedan R.V.: investigation, methodology, writing – review & editing.

Vladymyrskyi I.A.: formal analysis, funding acquisition, writing – review & editing.

Orlov A.K.: methodology, conceptualization, investigation, methodology, project administration, formal analysis, visualization, supervision, writing – review & editing.

Authors and CV

Oleksandr Palchekovskyi, Master Student, Junior Research Assistant, National Technical University of Ukraine "Igor Sikorsky Kyiv Polytechnic Institute". The area of scientific interests is investigation of electrophysical properties of metal thin films.
https:/orcid.org/0009-0002-6927-0351

Ivan Kruhlov, PhD, Senior Researcher, Senior Lecturer, National Technical University of Ukraine "Igor Sikorsky Kyiv Polytechnic Institute". The area of scientific interests is solid-state physics and ion irradiation of metal thin films.
E-mail: ivankruhlov@gmail.com,
https:/orcid.org/0000-0003-2078-4159

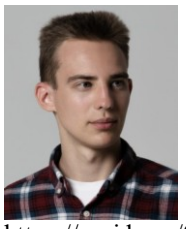

Roman Pedan, PhD student, Junior Researcher, National Technical University of Ukraine "Igor Sikorsky Kyiv Polytechnic Institute". The area of scientific interests is magnetic thin films and XRD analysis.
E-mail: roman1pedan@gmail.com,
https://orcid.org/0009-0004-9932-4079

Igor Vladymyrskyi, Professor, Doctor of Sciences, Senior Researcher, Director of the E.O. Paton Educational and Research Institute of Materials Science and Welding, National Technical University of Ukraine "Igor Sikorsky Kyiv Polytechnic Institute". The area of scientific interests is condensed matter physics and magnetic thin films.
E-mail: vladymyrskyi@kpm.kpi.ua,
https://orcid.org/0000-0002-2106-9176

Andrii Orlov, PhD, Senior Researcher, Associate Professor, National Technical University of Ukraine "Igor Sikorsky Kyiv Polytechnic Institute". The area of scientific interests is solid-state and experimental physics of thin-film materials.
E-mail: orlovandrii89@gmail.com,
https:/orcid.org/0000-0002-9219-3123

Структурна еволюція багатошарових Fe/Pt-плівок, відпалених у різних атмосферах: дослідження синхротронного випромінювання

О.А. Пальчековський, І.О. Круглов, Р.В. Педань, І.А. Владимирський, А.К. Орлов

Анотація. Досліджено вплив атмосфери відпалу на структурні властивості багатошарових тонких плівок $[Fe/Pt]_{\times 4}$ після відпалу. Плівки були нанесені на термічно окислені підкладки SiO_2(100нм)/Si(100) методом магнетронного розпорошення на постійному струмі за кімнатної температури, а потім відпалені в діапазоні температур від 500 до 900 °C у потоках атмосфер Ar, N_2 та $Ar + H_2$ для індукування структурних фазових переходів та хімічного впорядкування. Синхротронний аналіз показав, що впорядкована гранецентрована тетрагональна фаза $L1_0$-FePt утворюється після відпалу за температури 500 °C незалежно від використаної атмосфери. Серед досліджуваних умов відпал у N_2 за температури 800 °C забезпечив вищий ступінь хімічного впорядкування, сильну [001] кристалографічну текстуру та вищу тетрагональність фази $L1_0$-FePt, що робить її найбільш сприятливою для застосування в магнітному зберіганні даних. Шорсткість поверхні збільшується зі зростанням температури; однак її величина також залежить від атмосфери відпалу, залишаючись порівняно нижчою після відпалу в Ar порівняно з обробкою в реакційних середовищах, таких як N_2 або $Ar + H_2$. Крім того, разом з фазою $L1_0$-FePt відпал в атмосфері Ar сприяє утворенню нестехіометричного твердого розчину $Fe_{1+x}Pt_{3-x}$ та поверхневих оксидів ($Fe_3O_4 \rightarrow Fe_2O_3 \rightarrow FeO$).

Ключові слова: тонкі магнітні плівки, сплав Fe–Pt, синхротронне випромінювання, атмосфера відпалу, окислювальна поведінка.